A Theory of Joint Light and Heat Transport for Lambertian Scenes

Supplementary Material

A. Image Formation in a Thermal Camera

The field of Infrared Thermography is focused on recovering precise temperature measurements from the intensities recorded by a thermal camera. For an in-depth understanding of this subject, we refer the reader to [34]. In the following, we summarize the key concepts as pertaining to our system.

Let ϵ denote the emissivity of the object and T_n denote the corresponding surface temperature at time t_n. The corresponding intensity I_{thr} returned by an ideal thermal camera is written as

$$I_{thr}(t_n) = r_{bs}\bigg(\tau_{atm}\big(\epsilon U(T_n) + (1-\epsilon)U(T_{refl})\big) +$$
$$(1-\tau_{atm})U(T_{atm})\bigg) + \tau_{bs}U(T_{sys}) +$$
$$(1 - r_{bs} - \tau_{bs})U(T_{bs}), \tag{31}$$

where r_{bs}, τ_{bs}, and T_{bs} are the reflectivity, transmissivity and temperature of the beam splitter respectively. τ_{atm} and T_{atm} denote the transmissivity and temperature of the atmospheric medium between the camera and the object. T_{sys} is the effective temperature of the imaging system and T_{refl} is the effective temperature of radiation from the surrounding that is incident on the object. Note that the above expression, also called the radiometric chain, models the factors external to the camera, such as the different components of radiation that are incident at the lens of the thermal camera.

Factors internal to the camera, such as its operating temperature, lens characteristics, its type (microbolometer vs. cooled photon detectors), and sensor electronics, also influence the final intensity recorded by the camera. The resulting cumulative effect is modeled by the function U, called the radiometric function of the thermal camera.

In our experiment, we assume all components other than the object surface remain at constant temperature. This assumption is reasonable as our experiments are limited to short duration (< 3.5 seconds). Therefore Eq. (31) can be written as

$$I_{thr}(t_n) = \alpha U(T_n) + U_s \tag{32}$$
$$\text{where} \quad \alpha = r_{bs}\tau_{atm}\epsilon \tag{33}$$
$$U_s = r_{bs}\big(\tau_{atm}(1-\epsilon)U(T_{refl}) +$$
$$(1-\tau_{atm})U(T_{atm})\big) + \tau_{bs}U(T_{sys}) +$$
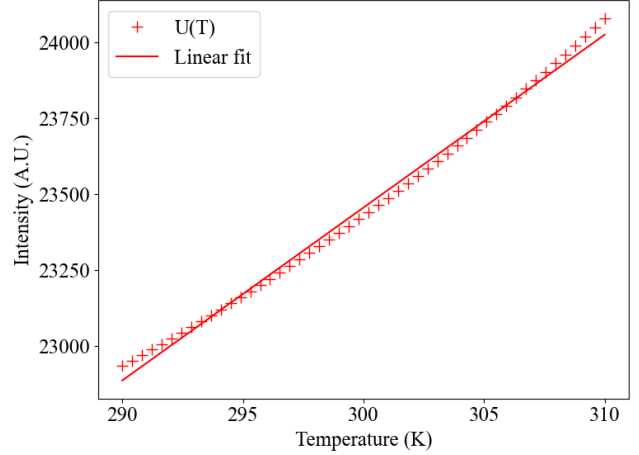$$(1 - r_{bs} - \tau_{bs})U(T_{bs}). \tag{34}$$

Figure 9. The radiometric function of a typical thermal camera for a small temperature range around room temperature. The linear fit defined with $T_* = 300$K introduces $< 0.2\%$ absolute error in intensity with respect to the mean pixel intensity in that temperature range.

A.1. Radiometric Function of Thermal Camera

The thermal camera's radiometric function U maps the temperature of a blackbody to the corresponding pixel intensity the camera would measure under ideal conditions. It is parameterized by the planckian form of the Sakumo-Hattori equations and is given by:

$$U(T) = \frac{R}{\exp(\frac{B}{T}) - F} + O, \tag{35}$$

where R, B, F and O are camera calibration parameters. Note that other forms of Sakumo-Hattori equations exist but the above expression is the one typically used by the camera manufacturer.

The function is typically defined over a broad range of temperatures, say $[-40°C, 150°C]$. However, the function can be linearized around a nominal temperature T_*. In all our experiments, the rise in pixel intensity due to light absorption was less than ≈ 1000 counts. Fig. 9 shows the plot of U for typical values of R, B, F, O and a small temperature range around room temperature. The linear fit defined around $T_* = 300$K agrees well with the non-linear function. The maximum error introduced due to linearization expressed as percentage of mean pixel intensity is 0.2%.

B. Analytical Solution to Eq. (7)

Eq. (7) from Sec. 3 can be written as

$$\frac{\partial T}{\partial t} = \frac{P(T_s - T)}{H} + \frac{S}{H}. \tag{36}$$

This can be written in standard form as

$$\int_{T_1}^{T_n} \frac{dT}{A - BT} = \int_{t_1}^{t_n} dt, \tag{37}$$

where $A = \frac{PT_s + S}{H}$ and $B = \frac{P}{H}$. The solution to this differential equation is written as

$$\frac{1}{-B} \log \left(\frac{A - BT_n}{A - BT_1} \right) = (t_n - t_1) \tag{38}$$

$$A - BT_n = (A - BT_1)e^{-B(t_n - t_1)} \tag{39}$$

Taking BT_n to the other side and subtracting BT_1 from both sides, we get

$$A - BT_1 = (A - BT_1)e^{-B(t_n - t_1)} + B(T_n - T_1) \tag{40}$$

$$B(T_n - T_1) = (A - BT_1)(1 - e^{-B(t_n - t_1)}) \tag{41}$$

Dividing both sides by B and substituting for A and B in the above equation, we get

$$T_n - T_1 = (\frac{S}{P} + T_s - T_1)(1 - e^{-\frac{P}{H}(t_n - t_1)}) \tag{42}$$

C. General Albedo, Flat Camera response

In applications with focus on shape or illumination, removing the effect of spatially varying albedo from the input image is a useful first step. In such cases, if we have a camera with a flat response across all wavelengths present in the illumination, we can derive a simple expression to directly compute the shading image.

Consider a monochrome camera with a constant spectral response such that $\Gamma(\lambda) = \Gamma_0 \; \forall \lambda$. This simplies Eq. (18) from Sec. 4 to

$$I(\mathbf{p}) = \frac{\gamma}{\pi}\Gamma_0 \int_\lambda \rho(\mathbf{x}, \lambda)L(\mathbf{x}, \lambda)d\lambda. \tag{43}$$

Combining Eq. (22) from Sec. 4 and Eq. (43), we can write

$$L(\mathbf{x}) = \int_\lambda L(\mathbf{x}, \lambda)d\lambda = \frac{\pi I(\mathbf{p})}{\gamma\Gamma_0} + \frac{\tilde{S}(\mathbf{x})}{\beta}, \tag{44}$$

where $L(\mathbf{x})$ is the total scene irradiance across all λ. Note that $L(\mathbf{x})$ contains all the information about shape and illumination. We have shown that it can be computed independent of albedo from a single view without any assumption about shape or illumination.

D. Computing E_k, F and L

Let $\Gamma_b(\lambda), \Gamma_g(\lambda)$, and $\Gamma_r(\lambda)$ be the sensor response functions corresponding to the BGR channels in the camera and let $l(\lambda)$ be the emission spectrum of the white LEDs obtained from the technical datasheets (see Fig. 2c). The wavelengths of interest can be partitioned into $\Lambda = \Lambda_B \cup \Lambda_G \cup \Lambda_R$, where $\Lambda_B = [400\text{nm}, 530\text{nm})$, $\Lambda_G = [530\text{nm}, 620\text{nm})$, and $\Lambda_R = [620\text{nm}, 1100\text{nm})$. Note that we include wavelengths in near infrared as well in our definitions since the sensor response functions are non-zero at those wavelengths.

Since $l(\lambda)$ is known, we can directly compute L as

$$L = \int_\Lambda l(\lambda)d\lambda. \tag{45}$$

In our experiments, we use $\Phi_\rho(\lambda) = \{\tilde{\rho}_b(\lambda), \tilde{\rho}_g(\lambda), \tilde{\rho}_r(\lambda)\}$ as the basis set for representing albedo as a function of wavelength. These basis functions are defined as

$$\tilde{\rho}_b(\lambda) = \mathbb{I}[\lambda \in \Lambda_B], \tag{46}$$

$$\tilde{\rho}_g(\lambda) = \mathbb{I}[\lambda \in \Lambda_G], \tag{47}$$

$$\tilde{\rho}_b(\lambda) = \mathbb{I}[\lambda \in \Lambda_R], \tag{48}$$

where $\mathbb{I}[\cdot]$ is the indicator function. Let $\mathbf{a_x} = \begin{bmatrix} \rho_b & \rho_g & \rho_r \end{bmatrix}^T$ be the corresponding vector of coefficients.

Since our basis functions are made up of indicator functions, their effective role is to restrict the integration limits in the definition of $\mathbf{E}_k$ and $\mathbf{F}$. We can now define these vectors as

$$\mathbf{E}_b = \begin{bmatrix} \int_{\Lambda_B} l(\lambda)\Gamma_b(\lambda)d\lambda & \int_{\Lambda_G} l(\lambda)\Gamma_b(\lambda)d\lambda & \int_{\Lambda_R} l(\lambda)\Gamma_b(\lambda)d\lambda \end{bmatrix} \tag{49}$$

$$\mathbf{E}_g = \begin{bmatrix} \int_{\Lambda_B} l(\lambda)\Gamma_g(\lambda)d\lambda & \int_{\Lambda_G} l(\lambda)\Gamma_g(\lambda)d\lambda & \int_{\Lambda_R} l(\lambda)\Gamma_g(\lambda)d\lambda \end{bmatrix} \tag{50}$$

$$\mathbf{E}_r = \begin{bmatrix} \int_{\Lambda_B} l(\lambda)\Gamma_r(\lambda)d\lambda & \int_{\Lambda_G} l(\lambda)\Gamma_r(\lambda)d\lambda & \int_{\Lambda_R} l(\lambda)\Gamma_r(\lambda)d\lambda \end{bmatrix} \tag{51}$$

$$\mathbf{F} = \begin{bmatrix} \int_{\Lambda_B} l(\lambda)d\lambda & \int_{\Lambda_G} l(\lambda)d\lambda & \int_{\Lambda_R} l(\lambda)d\lambda \end{bmatrix} \tag{52}$$

E. Grayscale Separation Results

Figure 10 summarizes the albedo shading separation results for the four target scenes using the grayscale approximation. Recall that the analytical expressions for the grayscale approximation are simpler and do not require knowledge of the emission spectrum or the camera response. Yet, as seen in the results, the estimated shading is similar to that obtained using the system of equations for general albedo functions.
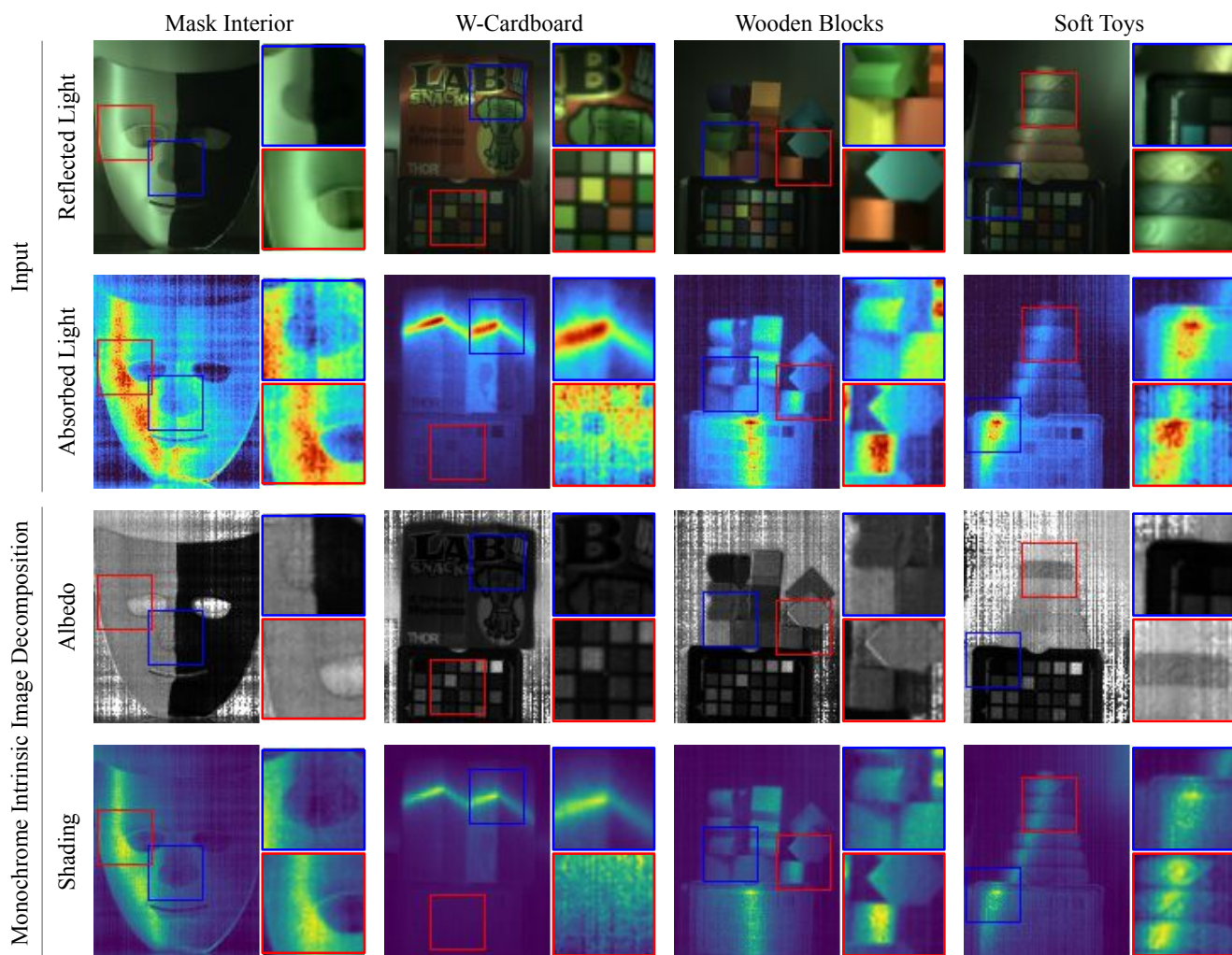
Figure 10. The first row shows the HDR visible image (brightened for visualization). Note that the colorchart is not an input to our method. The second row shows the estimated heat source intensity (turbo colormap) obtained using the method in Sec. 3. The last two rows correspond to using Eqs. (17) and Eqs. (16) respectively. The estimated albedo is clipped to the range $[0, 1]$. The callouts for the visible image, heat source intensity, and shading are normalized individually to aid visualization.